DOI: http://dx.doi.org/10.22104/ijhfc.2015.298

Iranian Journal of Hydrogen & Fuel Cell 4(2015) 263-270

Iranian Journal of Hydrogen & Fuel Cell

IJHFC

Journal homepage://ijhfc.irost.ir

Lattice Boltzmann Modeling of Two Component Gas Diffusion in a Solid Oxide Fuel Cell

Mohammad Reza Shahnazari[1,*], Khavar Fazeli[2]

[1]Faculty of Mechanical Engineering, K. N. Toosi University of Technology, Tehran, Iran.
[2]Department of Mechanical Engineering, University of California, Riverside, CA 92521, United States.

Article Information

Article History:

Received:
15 March 2016
Received in revised form:
30 May 2016
Accepted:
12 June 2016

Keywords

Gas flow
Porous media
Lattice Boltzmann method
Gas diffusion
Solid oxide fuel cell

Abstract

In recent years, the need for high efficiency, low emission power generation systems has focused much attention on the use of fuel cell technology. Solid oxide fuel cells are suitable for power generation systems due to their high operating temperature (800 °C -1000 °C).

Two-component gas flow (H_2 and H_2O) in the porous media of solid oxide fuel cell's anode have been modeled via the lattice Boltzmann method; molecular distributions of the components are evaluated and the concentration voltage drop is investigated. The results of the voltage drop in different current densities are validated with previous studies. Then the effects of various parameters, such as porosity and non-dimensional current density, on gas diffusion of H_2 and H_2O and also the concentration voltage drop in the porous anode are evaluated. It was revealed that at a specific non-dimensional current density, reducing porosity causes increasing H_2 concentration in the anode and concentration voltage loss. A computer program in MATLAB has been used to apply the CFD model.

1. Introduction

A fuel cell is a chemical cell that converts stored chemical energy in the fuel directly into electricity. In a fuel cell fuel is continuously injected into anode, and oxygen is injected into the cathode. Chemical reactions happen at the interface between the electrolyte and electrodes (TPB), and by creating electrical potential electricity will flow. The relationship between the anode and the cathode is provided through the electrolyte. Fuel cells are also categorized by the type of electrolyte.

A solid oxide fuel cell is a fuel cell with a solid physical structure, and all electrochemical reactions are performed in a two-phase gas-solid region. In the cathode, oxygen receives electrons from the external circuit. Then oxygen ions are transferred to the cathode through the electrolyte, and produce water at

*Corresponding Author's E-mail address: shahnazari@kntu.ac.ir

the interface of electrolyte and anode by reaction with hydrogen. The produced electrons flow to the cathode through an external circuit, and these reactions are repeated.

The solid oxide fuel cell anode is made of a porous material and due to the high temperature performance of this type of fuel cell, the reactive and production components remain in the gas phase. Thus, it is important to choose an appropriate method for modeling the gas diffusion phenomena. This paper presents a recently developed CFD model, called the Lattice Boltzmann Method (LBM) to investigate the transport phenomena of gas particles in the porous media of a solid oxide fuel cell's anode.

Lattice Boltzmann equations were used in CFD modeling for the first time in 1988. In the LBE method a series of averaging distribution functions are used, so in the initial model this method eliminates time-consuming steps of statistical averaging. In addition, using this simplified approach instead of complex operators leads to increased accuracy [1].

2. LB modeling

In this paper, the Nitiarasu et al. model was used for governing equations of fluid diffusion in porous material. This model is applicable for both constant and variable porosity. The continuity equation and generalized Navier Stoks for isothermal incompressible flows are expressed as follows [2], [3].

$$\nabla.\mathbf{u} = 0 \tag{1}$$

$$\frac{\partial \mathrm{u}}{\partial t} + \left(\mathrm{u}.\nabla\right)\left(\frac{\mathrm{u}}{\varepsilon}\right) = -\frac{1}{\rho}\nabla\left(\varepsilon p\right) + \upsilon_e \nabla^2 \mathrm{u} + \mathrm{F} \tag{2}$$

Where u and p are the mass flow rate and pressure, respectively, that are averaged in a Representative Elementary Volume (REV) of the flow domain. υ_e is the effective viscosity and F indicates the total volume of the porous material forces and other external force fields that are obtained from equation 3.

$$\mathrm{F} = -\frac{\varepsilon\upsilon}{K}\mathrm{u} - \frac{\varepsilon \mathrm{F}_\varepsilon}{\sqrt{K}}\left|\mathrm{u}\right|\mathrm{u} + \varepsilon \mathrm{G} \tag{3}$$

Where υ is the shear viscosity that is not necessarily equal to the effective viscosity υ_ε. G is the volume force that is obtained from the external force. F_ε is an experimental geometrical function that depends on the porosity and is defined as the following empirical equation 4 [3].

$$F_\varepsilon = \frac{1.75}{\sqrt{150\varepsilon^3}} \tag{4}$$

In the absence of porous material ($\varepsilon \rightarrow 1$), generalized momentum equation (2) becomes the Navier Stokes equation for free fluid flow.

The Method of Gunstensen et al. is also used for applying two-component gas diffusion. In this model, the Lattice Boltzmann method is applied in a way that it fulfills the generalized Navier-Stokes equations in porous media (equation (2)). For each of the species a separate distribution function, $f_a^{(k)}(x,t)$, is defined; the superscript k represents the different species (H_2 or H_2O). The Lattice Boltzmann equation for each component is as follows [3], [4].

$$f_a^{(k)}\left(\mathbf{x}+\mathbf{e}_a, t+1\right) = f_a^{(k)}\left(\mathbf{x},t\right) + F_a^{(k)} + \Omega_a^{(k)}\left(\mathbf{x},t\right) \tag{5}$$

Where $\mathrm{F_a^{(k)}}$ is the force term. To obtain the correct hydrodynamic equations, this force term is carefully selected and fluid velocity is modified accordingly. The best equation for fluid flows in porous media is as follows [4], [5].

$$F_a^{(k)} = \omega_a \rho^{(k)}\left(1 - \frac{1}{2\tau_k}\right)\times \left[\frac{\mathbf{e}_a.\mathbf{F}^{(k)}}{{c_s}^2} + \frac{\mathbf{u}^{(k)}\mathbf{F}^{(k)} : \left(\mathbf{e}_a\mathbf{e}_a - {c_s}^2\mathbf{I}\right)}{\varepsilon {c_s}^4}\right] \tag{6}$$

Where $F^{(k)}$ indicates the total volume forces acting on species k due to the existence of porous material and other external force fields. $F^{(k)}$ can be obtained from

the following equation [4].

$$\mathbf{F}^{(k)} = -\frac{\varepsilon \nu_k}{K}\mathbf{u}^{(k)} - \frac{\varepsilon \mathrm{F}_\varepsilon}{\sqrt{K}}\left|\mathbf{u}^{(k)}\right|\mathbf{u}^{(k)} + \varepsilon \mathbf{G}_k \quad (7)$$

Also, $\Omega_a^{(k)}$ in equation (5) is the collision term for the species k and represents the relaxationof the local equilibrium [4].

$$\Omega_a^{(k)} = \left(\Omega_a^{(k)}\right)^1 + \left(\Omega_a^{(k)}\right)^2 \quad (8)$$

The term $(\Omega_i^{(k)})^1$ in the above equation represents the same species collision [4], [6].

$$\left(\Omega_a^{(k)}\right)^1 = \frac{-1}{\tau_k}\left(f_a^{(k)} - f_a^{(k)eq}\right) \quad (9)$$

The term $(\Omega_i^{(k)})^2$ in equation (8) represents the different species collisions. In this paper, ideal gas mixture is assumed and different species collisions $(\Omega_i^{(k)})^2$ are neglected.

τ_k is the characteristic relaxation time for the species k, $f_i^{(k)eq}$ is its equilibrium distribution function and is obtained from the following equation [3], [4].

$$f_a^{(k)eq} = \omega_a \rho^{(k)}\left[1 + \frac{\mathbf{e}.\mathbf{u}^{(k)}}{{c_s}^2} + \frac{\mathbf{u}^{(k)}\mathbf{u}^{(k)} : \left(\mathbf{e}_i\mathbf{e}_i - {c_s}^2\mathbf{I}\right)}{2\varepsilon {c_s}^4}\right] \quad (10)$$

Where $\rho^{(k)}$ and $u^{(k)}$ are the macroscopic density and velocity of species k, respectively, and are obtained from the following equations [3], [4], [7], [8].

$$\rho^{(k)} = \sum_{a=0}^{8} f_a^{(k)} \quad (11)$$

$$\rho^{(k)}\mathbf{u}^{(k)} = \sum_{a=0}^{8}\mathbf{e}_a f_a + \frac{\delta_t}{2}\rho^{(k)}\mathbf{F}^{(k)} \quad (12)$$

Since $F^{(k)}$ includes the velocity term, the above equation is non-linear with respect to the speed term [3], [4].

$$\mathbf{u}^{(k)} = \frac{\mathbf{v}^{(k)}}{c_{0k} + \sqrt{{c_{0k}}^2 + c_1\left|\mathbf{v}^{(k)}\right|}} \quad (13)$$

$v^{(k)}$ is a parameter that is defined as follows [3], [4].

$$\mathbf{v}^{(k)} = \frac{1}{\rho^{(k)}}\left[\sum_{a=0}^{8}\mathbf{e}_a f_a^{(k)} + \frac{1}{2}\varepsilon\rho^{(k)}\mathbf{G}_k\right] \quad (14)$$

$v^{(k)}$ is called the temporary speed of species k due to its similarity with the speed relation in the simplified LB method. c_{0k} and c_1 are defined as follows [3], [4].

$$c_{0k} = \frac{1}{2}\left(1 + \varepsilon\frac{1}{2}\frac{\nu_k}{K}\right) \quad (15)$$

$$c_1 = \varepsilon\frac{1}{2}\frac{F_\varepsilon}{\sqrt{K}} \quad (16)$$

Where v_k is the kinematic viscosity of species k. Also, F_ε is obtained from equation (4). The state equation is $p=c_s^2\rho/\varepsilon$. The relationship between the effective viscosities and characteristic relaxation time is as follows [7].

$$\nu_e = c_s^2\left(\tau - 0.5\right)\delta_t \quad (17)$$

This equation relates viscosity of the fluid to the relaxation time. By applying the continuum and momentum conservation equation at each node, the total macroscopic velocity is obtained [4].

$$\mathbf{u} = \frac{1}{\rho}\sum_k \rho^{(k)}\mathbf{u}^{(k)} \quad (18)$$

Where ρ is the total density in each node and equals to the sum of the densities of all components at that node [4].

$$\rho = \sum_k \rho^{(k)} \quad (19)$$

3. Theory

One of the main parameters of a fuel cell is the current density (i). The relationship between current density and the molar flux in the TPB is defined by the following equation.

$$i = 2Fj \quad (20)$$

Another important parameter of gas flow in the electrode is non dimensional flux (J^*) which is defined as follows [9].

$$J^* = \frac{JL}{C_T D} \tag{21}$$

Where C_T is the total molar concentration and D a collision factor between the two species. The amount of J^* in a solid oxide fuel is small and it is typically in the range of 10^{-2}. In this paper, this parameter is used as a characteristic parameter for comparison of fuel cell specifications. Also, the non-dimensional current density (i^*) is equal to the non-dimensional flux (J^*) [9].

$$i^* = \frac{iL}{2FC_T D} = J^* \tag{22}$$

The concentration voltage drop is obtained by the following equation [9], [10].

$$\eta_{conc} = E_{in\ surface\ of\ electrod} - E_{in\ TPB} \tag{23}$$

In this equation E is the Nernst voltage that is obtained from the following equation with respect to the species mole fraction (or partial pressure) [11].

$$E = E^0 + \frac{RT}{2F} \ln\left[\frac{P_{H_2} P_{O_2}{}^{0.5}}{P_{H_2O}}\right] \tag{24}$$

The geometry of a solid oxide fuel cell anode is considered as a computational domain, and the steady state fluid flow of the two-component gas (H_2 and H_2O) is modeled. Since the gas diffusion in the cathode is not modeled, the partial pressure of the O_2 in all parts of the cathode is considered to be constant. By using the results of this numerical simulation, the concentration polarization of the anode is calculated in various current densities.

The isothermal condition assumed in the anode and diffusion parameters are constant. Also, the working pressure of the cell is 1 atm. The mixture is considered as an ideal gas and the partial pressures of each gas component equals to its mole fraction. In order to simplify the model, very thin TPB area is considered [9].

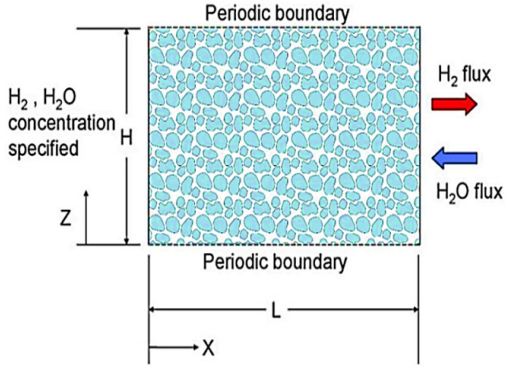

Fig. 1. 2D model of SOFC anode [9].

At the fuel channel (surface of the anode), the mole fractions of H_2 and H_2O are considered to be 0.97 and 0.03, respectively. Therefore, the Dirichlet boundary condition is applied at x = 0 for both species [7], [12]. Since the cell parameters are specified in different current densities, molar flux of H_2 (and subsequently H_2O) in the TPB can be obtained. Hence, the Neumann boundary conditions are applied for both H_2 and H_2O at x = L.[7], [13]. In order to increase the computing efficiency, the height H of the field is considered by reasonable size. Herein a square field (H = L) is assumed and at z = 0 and z = H the periodic boundary conditions is applied [14], [15], [9]. The CFD model has the following characteristics.

- The lattice size is 150 × 150.
- Gas flow in the porous anode consists of two components (H_2 and H_2O).
- The initial mole fraction of each of the components is considered to be uniform over the computational field and equal to the mole fraction of components in the fuel channel (electrode surface).
- The initial velocity of all components is considered zero at all nodes and the initial distribution functions are assumed to be equal to the weighting function (ω_a).

4. Presentation of results

In this section, the obtained polarization density values of the fuel cell are compared with previous studies by Chan et al. and Zhao and Virkar [16], [17].

Also, the H_2 mole fraction change in the TPB and concentration polarization obtained from LBM have been reviewed at various porosity of the anode and the corresponding graphs are plotted.

Chan et al. presented a solid oxide fuel cell model based on empirical relationships in terms of current density and plotted the anode concentration polarization curves. Zhao and Virkar also presented the concentration polarization curves of the anode versus current density by using empirical models.

To be able to compare the results with previous studies, the parameters should be uniformed. For example, according to relations (20) to (22), the current density (i) in previous studies becomes to the non-dimensional current density(i^*).

After LBM modeling, according to the known mole fractions of gases H_2 and H_2O in TPB and using the relations (23) and (24), values of concentration polarization are calculated. Concentration polarization curves are plotted in terms of non-dimensional current density and are compared with previous results.

Chan et al. provided the following characteristics data [16]:

- Porosity = 30%, tortuosity = 6, and L = 750 × 10^6 m.
- The binary diffusivity value D = 1.085×104 ($m^2.s^{-1}$).
- The total molar concentration C_T=11.4 ($mol.m^{-3}$).
- The pressure is 1 atm and the temperature is 1073 K.

Note that the Tortuosity is not a LBM model parameter, but in Chan et al., Zhao and Virkar, and many other studies on one-dimensional models of porous material, it is applied as an empirical parameter for converting the collision coefficients. Tortuosity varies depending on the microstructures of porous media. Zhao and Virkar studies had a porosity of 32%, which is close to Chan et al.'s 30% [16], [17].

In Figure (2) the graph of concentration polarization of the LBM model is compared with previous studies. LBM results are plotted in the porosity of 30%. As you can see, the curve of concentration polarization of LBM is fairly close to the other two models. Visible differences between the predicted concentrations in the LBM model and previous studies may be due to the assumption of ideal mixture, two-dimensional geometry of LBM, discontinuity effects, and experimental parameters used in previous models, such as Tortuosity.

In Figures (3) and (4) the mole fraction of H_2 and H_2O in the anode with porosity of 40% and non-dimensional current density of 0.096 is shown, respectively. Large non-dimensional current density is selected in order to clearly show the differences in the mole fraction of components. Since H_2 is consumed in the TPB, its mole fraction in the TPB is less than the fuel channel. Similarly, because of the production of H_2O in TPB, its mole fraction in this region is higher than other areas in the anode.

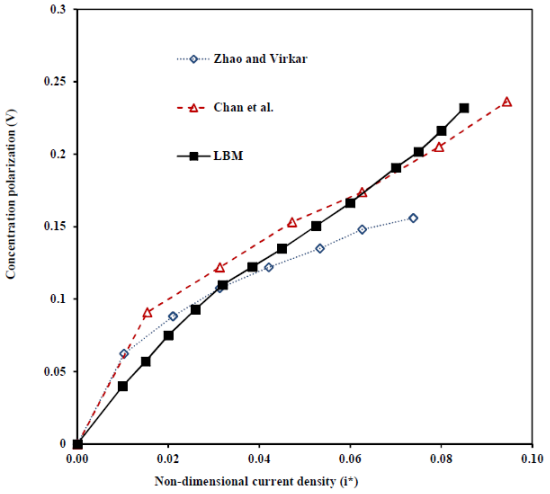

Fig. 2. Comparison of concentration polarization curves of LMB with previous studies [16] and [17] with a porosity of 30%.

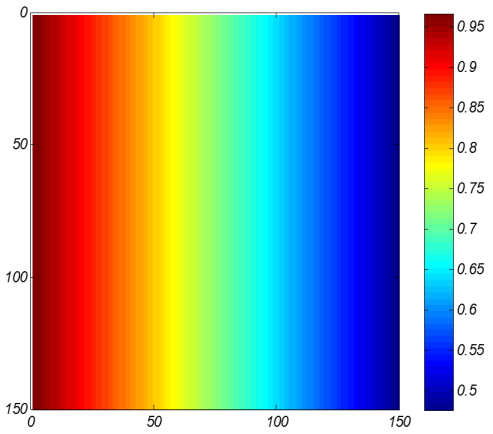

Fig. 3. Mole fraction of H_2 in the anode with porosity of 40% and the non-dimensional current density of 0.096.

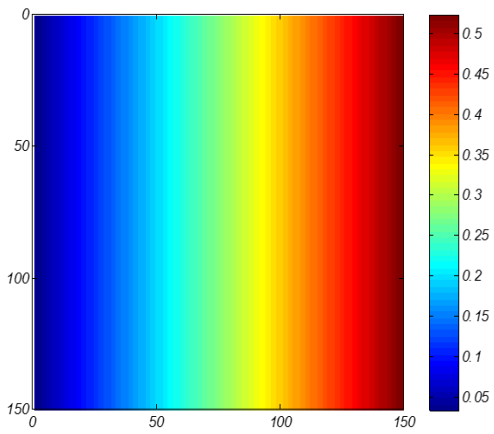

Fig. 4. Mole fraction of H_2O in the anode with porosity of 40% and the non-dimensional current density of 0.096.

Reducing the anode porosity leads to less available gas flow channels in the porous material. This will affect the gas diffusion process in the anode. In Figure (5), the effect of change in porosity on H_2 mole fraction in the TPB area is plotted for different non-dimensional fluxes. In all curves, the H_2 mole fraction at x = 0 is equal to 0.97.

The following results can be obtained from Figure (5).

- At a certain non-dimensional flux, as the porosity decreases the slope of changes in H_2 concentration increases and if the mole fraction of H_2 at x = 0 is kept constant, by reducing the porosity, the H_2 mole fraction decreases in TPB.
- At a given porosity, by increasing non-dimensional flux the slope of changes in H_2 mole fraction increases and the H_2 mole fraction decrease in TPB.

In Fuel cells a low concentration of fuel in the TPB results in a high concentration polarization voltage drop in the anode, and in low porosities and large non-dimensional fluxes the voltage drop is even larger. In this study, the concentration polarization voltage drop was calculated in different non-dimensional current density (i^*) and porosities, as shown in the diagram in Figure (6). The general trend of the anode concentration polarization curve is similar in different porosities. The results obtained from these curves can be summarized as follows.

- At a certain non-dimensional current density (i^*), the concentration polarization increases by when the porosity decreases. The reason for this is that the mole fraction of H_2 in the TPB decreases in low porosities.
- The polarization curve has a higher slope in lower porosities. This means that concentration polarization

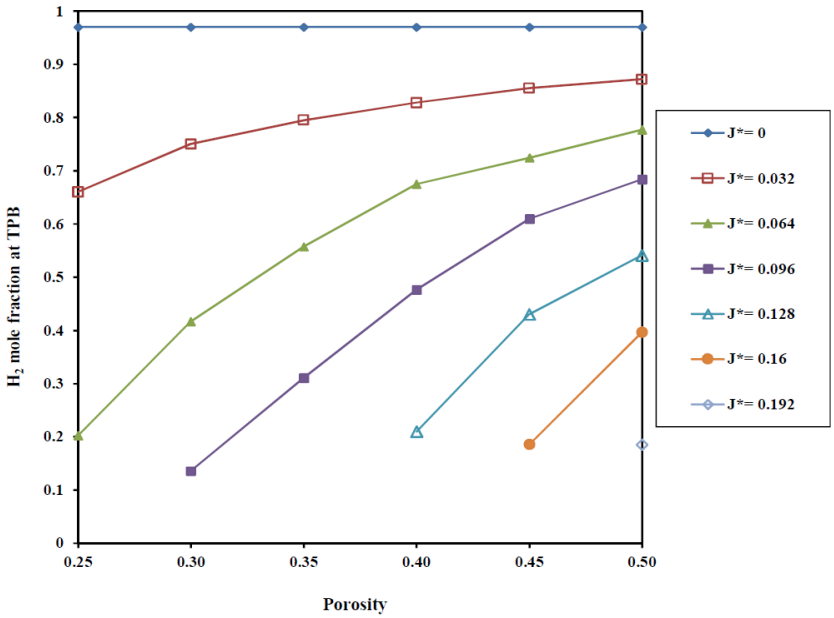

Fig. 5. The effect of porosity and non-dimensional flux on the mole fraction of H_2 in the anode TPB.

is more sensitive to changes in current density in low porosities.

- For the last plotted point, the mole fraction of H_2 in the TPB is zero meaning Limiting Current happened. Also, some of the curves at high current density cannot be plotted.
- In low porosities, the maximum current production capacity of the SOFC is lower than for high porosities.

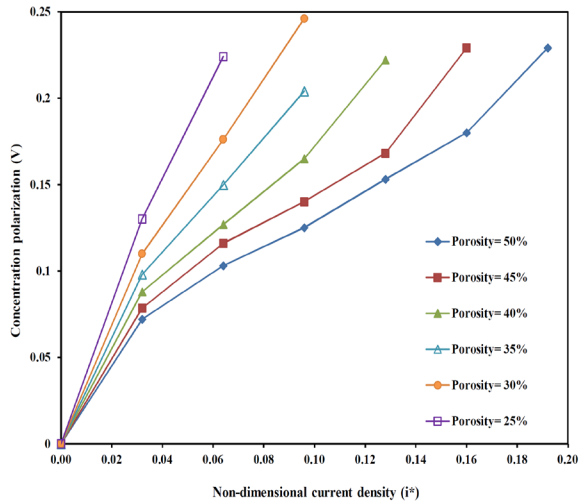

Fig. 6. concentration polarization voltage drop in different non-dimensional current density and porosities.

As can be seen from the graphs, porosity leads to a better penetration of fuel thereby reducing the concentration polarization. However, in high porosity the electrochemical reaction areas as well as the pathway for electron flow decrease at the anode resulting in higher activation and ohmic losses (which are not modeled here) at the anode [11]. Also, by increasing the porosity the mechanical strength decreases. There is always an optimum porosity where the total polarization losses are minimized. In practice, usually the anode structure is designed in a way that the porosity close to the gas channel is relatively higher than the electrolyte. This increases the active surface for chemical reaction at the anode and balances the voltage drops [9].

5. Discussion and conclusion

The diffusion of H_2 and H_2O has been modeled acceptably using the Lattice Boltzmann method. Applying this method in modeling the mass transport in SOFC anode is relatively successful and it can be an efficient tool in the study of fuel cells.

The results for SOFC anode concentration polarization are in good agreement with previous studies in middle range non-dimensional current density values, but in non-dimensional current densities less than 0.03 and greater than 0.075 there is a slight difference between LB results and previous studies. This may be due to differences in modeling techniques, assumptions, and parameters used for each method. In the LBM, an ideal mixing is assumed since modeling non-ideal mixture requires adding complex terms and relationships for unequal particles. However, this simplification was not considered in previous models.

Also, two-dimensional modeling was carried out in this paper, whereas previous studies were based on one-dimensional models. Additionally, empirical parameters such as Tortuosity were considered in previous studies, but there is no possibility of applying this parameter in the LB model.

6. References

[1] Rothman DH, Keller JM., Immiscible cellular-automaton fluids, J. Stat. Phys. 52: 1119–27, 1988.

[2] P. Nithiarasu, K.N. Seetharamu, and T. Sundararajan, Int. J. Heat Mass Transf. 40, 3955 (1997).

[3] Z. Guo, T.S. Zhao, Lattice Boltzmann model for incompressible flows through porous media, Phys. Rev. E 68 (2003) 035302.

[4] S. Chen & G. D. Doolen, Lattice Boltzmann method for fluid flows, A. Rev. Fluid Mech. 30, (1998) 329-74.

[5] Z. Guo, C. Zheng, and B. Shi, Phys. Rev. E 65, 046308, 2002.

[6] H. Hayashi, Lattice Boltzmann method end its aplication to flow analysis in porous media, R&D Review of toyota CRDL Vol.38, 2007.

[7] M. C. Sukop, D. T. Thorne, Lattice Boltzmann modeling An introduction for geoscientists and engineers.

[8] R. R. Nourgaliev et al., The Lattice Boltzmann Equation Method: Theoretical Interpretation, Numerics and Implications, Center for Risk Studies and Safety, University of California.

[9] A. S. Joshi, K. N. Grew, A. A. Peracchio, W. K. S. Chiu, Lattice Boltzmann modeling of 2D gas transport in a solid oxide fuel cell anode, J. Power Sources 164 (2007) 631–638.

[10] B. Sunden and M. Faghri, Transport phenpmena in fuelcells, WITPRESS, 2005.

[11] R. O'Hayre, S-W. Cha, W. Colella and F. B. Prinz, Fuel cell fundamentals, John Wiley & Sons, Inc, 2009.

[12] Q. Zou and X. He, Pressure and Velocity boundary conditions for the lattice Boltzmann BGK model, Phys. Fluids. 9, 1591-1598, 1997.

[13] S. Chen, D. Martinez, On boundary conditions in lattice Boltzmann methods, Phys. fluids. 8, 2527-2536, 1996.

[14] D. A. Wolf-Gladrow, Lattice-Gas cellular automata and Lattice Boltzmann models an introduction, Springer, 2005.

[15] M. C. Sukop, D. T. Thorne, Lattice Boltzmann modeling an introduction for geoscientists and engineers.

[16] S.H. Chan, K.A. Khor, Z.T. Xia, A complete polarization model of a solid oxide fuel cell and its sensitivity to the change of cell component thickness, J. Power Sources 93 (2001) 130–140.

[17] F. Zhao, A.V. Virkar, Dependence of polarization in anode-supported solid oxide fuel cells on various cell parameters, J. Power Sources 141 (2005) 79–95.